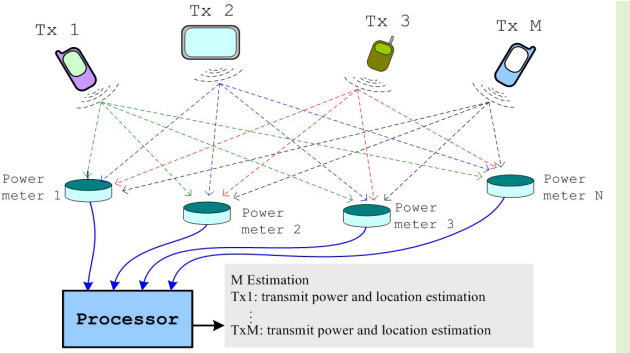


Advanced RSS-Based Multisource Localization: Sequential Hypothesis Testing for Robust Location Estimation

Hamid Katabalian^{ID}, Mehrzad Biguesh^{ID}, and Abbass Sheikhi^{ID}

Abstract—Accurate estimation of the number, locations, and transmit powers of wireless signal sources is crucial for various applications, including surveillance and monitoring. In this article, we propose a novel algorithm based on received signal strength (RSS) measurements to address this problem. Our approach utilizes sequential binary hypothesis testing, offering a computationally efficient solution without prior knowledge of the number of sources. Through extensive simulations, we demonstrate the superior performance of our algorithm compared with the existing methods, such as exhaustive search and multiresolution (MR) search, in terms of accuracy and computational complexity. Notably, our algorithm exhibits robustness in scenarios with multiple sources and close proximity between them. We also conduct performance analysis to evaluate its sensitivity to noise variance and false alarm probability, showcasing its reliability under different conditions. Our work contributes to advancing wireless signal processing techniques and offers promising implications for enhanced surveillance and monitoring capabilities in wireless communication systems. Overall, our proposed algorithm presents an efficient and accurate solution for estimating wireless signal sources, with potential for significant impact on practical applications.

Index Terms—Location fixing, maximum likelihood (ML), multisource localization, received signal strength (RSS), sequential hypothesis test, source enumeration.



I. INTRODUCTION

SOURCE localization, also known as source location fixing, has garnered considerable attention across various domains, including wireless networks [1], wireless sensor networks [2], [3], mobile localization [4], sonar [5], radar [6], [7], teleconferencing [8], robotics [9], cognitive radio, navigation, emergency services, and smart traffic control.

Numerous techniques have been developed for this purpose, employing methodologies, such as time of arrival (TOA) and time difference of arrival (TDOA) [10], [11], [12], [13], frequency difference of arrival (FDOA) [14], angle of arrival (AOA) [15], [16], [17], [18], [19], received signal strength (RSS) and differential RSS (DRSS) [20], [21], [22], [23],

Received 31 July 2024; revised 11 September 2024; accepted 13 September 2024. Date of publication 24 September 2024; date of current version 14 November 2024. This work was supported by the Research Vice-Presidency of Shiraz University under Grant 2007-208. The associate editor coordinating the review of this article and approving it for publication was Dr. Engin Masazade. (*Corresponding author: Mehrzad Biguesh.*)

The authors are with the Department of Communications and Electronics Engineering, School of Electrical and Computer Engineering, Shiraz University, Shiraz 71348-51154, Iran (e-mail: hamidkatabalian@shirazu.ac.ir; biguesh@shirazu.ac.ir; sheikhi@shirazu.ac.ir).

Digital Object Identifier 10.1109/JSEN.2024.3463542

[24], [25], or a combination of these measurements [26], [27], [28]. Among these, measuring the power of the received signal stands out as a simple and cost-effective implementation process, making RSS-based localization an attractive solution compared with other methods.

Several approaches have been proposed for single-source localization using RSS measurements, including maximum likelihood (ML) [29], semidefinite relaxation (SDR) [30], [31], and the weighted least squares (WLS) method [32], [33], [34]. While the ML method offers high localization accuracy, its nonlinear cost function makes it sensitive to initial conditions, potentially leading to divergence. SDR techniques approximate the nonconvex ML problem to a convex one to ensure convergence but at the expense of increased computational complexity. Similarly, WLS-based methods simplify computations by converting RSS measurements into linear equations, but unbiased estimation of sensor distances from the source remains a challenge [35].

For multisource localization based on RSS measurements, the ML algorithm is widely employed despite its computational complexity. Alternative methods, such as multiresolution (MR) search [36] and expectation–maximization (EM) algorithms [37], have been proposed, each with its

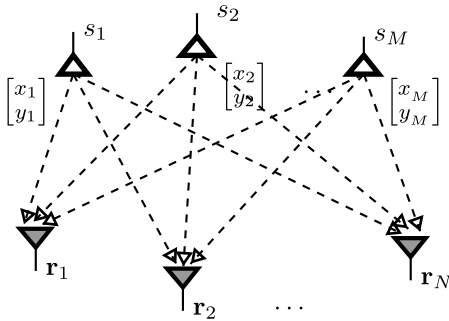


Fig. 1. System with N sensors at known locations and M sources.

strengths and limitations. However, these methods typically require prior knowledge of the number of sources, posing a significant challenge in real-world scenarios.

Methods for source number estimation, such as the minimum description length (MDL) method [38], [39] and the Akaike information criterion (AIC) [40], have shown promise but may exhibit poor detection performance with limited data. Other techniques, such as CLEAN, originally developed for radio astronomy [41], [42], have been adapted for source localization with varying degrees of success.

In this article, we propose an algorithm based on sequential generalized likelihood ratio testing (GLRT) to jointly estimate the location and number of sources. In addition, we derive an analytical performance bound for correct source number estimation, demonstrating the algorithm's efficacy, particularly in scenarios with closely spaced sources.

The remainder of this article is organized as follows. Section II describes the system model, while Section III presents our proposed method for joint source detection and location estimation. In Section IV, we analyze an analytical performance bound for the probability of correct source number estimation. Simulation results are provided in Section V, followed by a comparative study of computational complexity in Section VI. Finally, we conclude our findings in Section VII.

In this article, matrices are denoted by upper boldface letters, and vectors are represented by lower boldface letters. The symbol \mathbf{I}_n denotes the n -dimensional identity matrix, $|\cdot|$ represents the absolute value, and $\|\cdot\|$ denotes the Euclidean norm of a vector. The superscript T denotes the transpose of a matrix or vector, $\Pr\{\cdot\}$ indicates probability, and $E\{\cdot\}$ stands for the mathematical expectation.

II. SYSTEM MODEL

We assume a scenario where N receiver stations with known locations are distributed over a 2-D surveillance area in which $M < N$ independent sources are located in unknown locations (see Fig. 1). The 2-D vectors $\mathbf{r}_i = [\beta_i \ \gamma_i]^T$ for $1 \leq i \leq N$ denote the i th sensor's location. It is assumed that the received signal from the sources cannot be separated in time, frequency, or code space, and $[x_k \ y_k]^T$ for $1 \leq k \leq M$ is the location vector of the sources.

In a wireless environment, we can model the average received signal power¹ at the i th sensor from the M

¹We have to stress that this is the average of the instantaneous received power, which may undergo different types of fast fading.

noncoherent signal sources as follows [36], [37], [43], [44]²:

$$P_i = g_i \sum_{k=1}^M \frac{s_k}{(d_{ik})^\alpha} + v_i, \quad \text{for } i = 1, \dots, N \quad (1)$$

where $d_{ik} = ((\beta_i - x_k)^2 + (\gamma_i - y_k)^2)^{1/2}$ is the distance between the i th sensor and the k th signal transmitter, g_i is the gain factor of the i th sensor (assumed to be 1 without loss of generality), s_k denotes the signal strength at some reference distance d_o from the k th source, α is the path loss exponent, and the values of v_i represent measurement errors or modeling inaccuracies, which we assume to have an identically distributed Gaussian distribution with mean \bar{v} and variance σ_v^2 . In addition, since we use independent measuring sensors, these errors are also independent.³

If we define $p_i \stackrel{\text{def}}{=} P_i - \bar{v}$ as the i th station *observed power*, the probability density function (pdf) of the observed power vector $\mathbf{p} \stackrel{\text{def}}{=} [p_1 \ \dots \ p_N]^T$ is

$$f_{\mathbf{p}}(\mathbf{p}|\theta) = \prod_{i=1}^N \frac{1}{\sqrt{2\pi\sigma_v^2}} e^{-\frac{1}{2\sigma_v^2}(p_i - \sum_{k=1}^M \frac{s_k}{(d_{ik})^\alpha})^2} \quad (2)$$

where $\theta = [x_1 \ y_1 \ \dots \ x_M \ y_M \ s_1 \ \dots \ s_M]^T$ is the unknown vector parameter.

III. PROPOSED METHOD

The objective of this article is to estimate the number of sources M , the source's locations $(x_1, y_1), \dots, (x_M, y_M)$, and transmit powers s_1, \dots, s_M , based on the observed powers p_1, \dots, p_N . To accomplish this goal, we utilize a sequential hypothesis testing procedure [45], [46], [47] as a sequential detection and estimation algorithm for inferring the unknown parameters.

We formulate the problem by stacking p_1, \dots, p_N into the vector \mathbf{p} and establishing a matrix relation given by

$$\mathbf{p} = \mathbf{D}_M \mathbf{s}_M + \mathbf{w}. \quad (3)$$

Here, $\mathbf{D}_M = [\mathbf{d}_1 \ \dots \ \mathbf{d}_M]$ denotes the $N \times M$ dimensional distance matrix, consisting of vectors $\mathbf{d}_k = [d_{1k}^{-\alpha} \ \dots \ d_{Nk}^{-\alpha}]^T$, representing the distances from the k th signal transmitter to the N measuring points. In addition, $\mathbf{s}_M = [s_1 \ \dots \ s_M]^T$, and $\mathbf{w} = [(v_1 - \bar{v}) \ \dots \ (v_N - \bar{v})]^T$ represents the observation error, which follows a normal distribution $\mathcal{N}(\mathbf{0}, \sigma_v^2 \mathbf{I}_N)$.

Since matrix \mathbf{D}_M and vector \mathbf{s}_M are deterministic, the distribution of the observation vector \mathbf{p} will also be Gaussian, and its covariance matrix will be $\sigma_v^2 \mathbf{I}$. To estimate the sources' powers, locations, and their numbers, we propose employing a sequential hypothesis testing approach.

²We have to mention that the system performance is superior if signal bandwidth is known. In this way, relative error is minimized, and the location error will be decreased.

³The impact of environmental obstacles is crucial in determining the nature of the localization error. Obstacles, such as building materials and vegetation, affect the received signal strength, which, in turn, impacts source localization. Variability in RSS due to these environmental factors increases modeling error, thereby affecting the overall accuracy of the localization process. In addition, if the system bandwidth exceeds the signal bandwidth, the excess system noise increases the mean error, denoted as \bar{v} .

At each step m of our proposed sequential hypothesis testing, we assess the hypothesis test problem⁴

$$\begin{cases} H_{0,m} : \mathbf{p} = \mathbf{D}_{m-1}\mathbf{s}_{m-1} + \mathbf{w} \\ H_{1,m} : \mathbf{p} = \mathbf{D}_m\mathbf{s}_m + \mathbf{w}. \end{cases} \quad (4)$$

Problem (4) is a composite hypothesis problem with the unknown parameters x_m , y_m , and s_m . We employ the generalized likelihood ratio (GLR)-based detector to solve this composite hypothesis problem.⁵

The likelihood ratio $L_m(\mathbf{p})$ and the estimated value of s_m are provided as follows (refer to Appendix A for detailed derivations):

$$L_m(\mathbf{p}) = \max_{x_m, y_m} \frac{|\mathbf{d}_m^T \mathbf{D}_{m-1}^\perp \mathbf{p}|^2}{\mathbf{d}_m^T \mathbf{D}_{m-1}^\perp \mathbf{d}_m} \stackrel{H_{1,m}}{\gtrless} \eta_m \quad (5)$$

$$\hat{s}_m = \frac{\mathbf{d}_m^T \mathbf{D}_{m-1}^\perp \mathbf{p}}{\mathbf{d}_m^T \mathbf{D}_{m-1}^\perp \mathbf{d}_m} \quad (6)$$

where the significance level η_m is determined based on the required false alarm probability at the m th step $P_{fa}^{(m)}$ and \mathbf{D}_m^\perp is the orthogonal complement of \mathbf{D}_m , computed as follows:

$$\mathbf{D}_m^\perp = \begin{cases} \mathbf{I}_N - \mathbf{D}_m (\mathbf{D}_m^T \mathbf{D}_m)^{-1} \mathbf{D}_m^T, & m > 0 \\ \mathbf{I}_N, & m = 0. \end{cases} \quad (7)$$

For $m = 1$, we commence with the following test:

$$\begin{cases} H_{0,1} : \mathbf{p} = \mathbf{w} \\ H_{1,1} : \mathbf{p} = \mathbf{d}_1 s_1 + \mathbf{w}. \end{cases} \quad (8)$$

Hypothesis $H_{0,1}$ implies the absence of any source in the region, treating the measurements as noise, while $H_{1,1}$ suggests the existence of one or a transmitting object in the coverage area. If one or more sources exist in the scenario, $H_{1,1}$ provides a better fit to the model. In this case, we have

$$L_1(\mathbf{p}) = \max_{(x_1, y_1)} \frac{|\mathbf{d}_1^T \mathbf{p}|^2}{\|\mathbf{d}_1\|^2} > \eta_1$$

and, in this case, s_1 is estimated as $\hat{s}_1 = (\mathbf{d}_1^T \mathbf{p}) / (\|\mathbf{d}_1\|^2)$.

To estimate the number and location of the sources, we begin with $m = 1$ and increase m sequentially as long as hypothesis $H_{1,m}$ is valid.

The main steps of the our proposed algorithm are outlined in Table I.

IV. PERFORMANCE ANALYSIS

The pseudo-clairvoyant detector derived in Appendix A is used in order to calculate a bound for the probability of correctly detecting the number of sources, M . The probability of correctly detecting the number of sources P_c by assuming the presence of M sources is given by

$$P_c = \Pr \left\{ \left\{ \bigcap_{k=1}^M \{L_k(\mathbf{p}) > \eta_k\} \right\} \cap \{L_{M+1}(\mathbf{p}) < \eta_{M+1}\} \right\}. \quad (9)$$

⁴The extra subscript m in hypotheses H_0 and H_1 denotes the hypotheses at the m th step of the proposed algorithm.

⁵ \mathbf{D}_0 and \mathbf{s}_0 are set to zero.

TABLE I
OVERVIEW OF THE PROPOSED SEQUENTIAL HYPOTHESIS TESTING STEPS

Step 1	Take the received powers P_1, \dots, P_N as inputs.
Step 2	Compute $\mathbf{p} = [(P_1 - \bar{v}) \ \dots \ (P_N - \bar{v})]^T$
Step 3	$k = 1, \hat{\theta} = []$, $\mathbf{D}_0 = \mathbf{0}$, $\mathbf{D}_0^\perp = \mathbf{I}_N$
Step 4	Compute η_k based on the desired $P_{fa,k}$
Step 5	$L_k(\mathbf{p}) = \max_{(x_k, y_k)} \frac{ \mathbf{d}_k^T \mathbf{D}_{k-1}^\perp \mathbf{p} ^2}{\mathbf{d}_k^T \mathbf{D}_{k-1}^\perp \mathbf{d}_k}$
Step 6	if $L_k(\mathbf{p}) > \eta_k$: Go to step 7 if $L_k(\mathbf{p}) < \eta_k$: $k \leftarrow (k - 1)$, Go to step 8
Step 7	$(\hat{x}_k, \hat{y}_k) = \arg \max_{(x_k, y_k)} \frac{ \mathbf{d}_k^T \mathbf{D}_{k-1}^\perp \mathbf{p} ^2}{\mathbf{d}_k^T \mathbf{D}_{k-1}^\perp \mathbf{d}_k}$ $\hat{s}_k = \frac{\mathbf{d}_k^T \mathbf{D}_{k-1}^\perp \mathbf{p}}{\mathbf{d}_k^T \mathbf{D}_{k-1}^\perp \mathbf{d}_k}$ $\mathbf{D}_k = [\mathbf{D}_{k-1} \ \mathbf{d}_k]$ $\mathbf{D}_k^\perp = \mathbf{I} - \mathbf{D}_k (\mathbf{D}_k^T \mathbf{D}_k)^{-1} \mathbf{D}_k^T$ $k \leftarrow (k + 1)$ Go to Step 4.
Step 8	$M \leftarrow k$ $\hat{\theta} = [\hat{x}_1 \ \hat{y}_1 \ \dots \ \hat{x}_M \ \hat{y}_M \ \hat{s}_1 \ \dots \ \hat{s}_M]^T$

In Appendix B, we have shown that $L_i(\mathbf{p})$ and $L_j(\mathbf{p})$ are independent for $i \neq j$; as a result, (9) can be written as follows:

$$P_c = \Pr\{L_{M+1}(\mathbf{p}) < \eta_{M+1}\} \prod_{k=1}^M \Pr\{L_k(\mathbf{p}) > \eta_k\}. \quad (10)$$

In Appendix C, we have discussed that $z_i \stackrel{\text{def}}{=} (\mathbf{d}_i^T \mathbf{D}_{i-1}^\perp \mathbf{p}) / ((\mathbf{d}_i^T \mathbf{D}_{i-1}^\perp \mathbf{d}_i)^{1/2})$ follows a normal distribution, given by $z_i \sim \mathcal{N}(\mu_i, \sigma_v^2)$, where μ_i is defined as follows:

$$\mu_i = \begin{cases} \frac{\sum_{k=i}^M s_k \mathbf{d}_k^T \mathbf{D}_{i-1}^\perp \mathbf{d}_k}{\sqrt{\mathbf{d}_i^T \mathbf{D}_{i-1}^\perp \mathbf{d}_i}}, & \text{for } i \leq M \\ 0, & \text{for } i = M + 1. \end{cases}$$

Since $L_i(\mathbf{p}) = z_i^2$, we have

$$\Pr\{L_i(\mathbf{p}) < \eta_i\} = \Pr\{z_i^2 < \eta_i\} = 1 - 2Q\left(\frac{\sqrt{\eta_i}}{\sigma_v}\right) \quad (11)$$

$$\begin{aligned} \Pr\{L_i(\mathbf{p}) > \eta_i\} &= \Pr\{z_i^2 > \eta_i\} \\ &= Q\left(\frac{\sqrt{\eta_i} + \mu_i}{\sigma_v}\right) + Q\left(\frac{\sqrt{\eta_i} - \mu_i}{\sigma_v}\right) \end{aligned} \quad (12)$$

where $Q(\cdot)$ is the Gaussian Q function.

The probability of correct detection at the algorithm i th step is $P_{ci} = \Pr\{L_i(\mathbf{p}) > \eta_i; H_{1,i}\}$, and the probability of false alarm at this step is $P_{fa_i} = \Pr\{L_i(\mathbf{p}) > \eta_i; H_{0,i}\}$, where using (11), we have

$$P_{fa_i} = 2Q\left(\frac{\sqrt{\eta_i}}{\sigma_v}\right). \quad (13)$$

Therefore, at the presence of M sources, the probability of correct detection would be

$$\begin{aligned} P_c &= \left(1 - 2Q\left(\frac{\sqrt{\eta_{M+1}}}{\sigma_v}\right)\right) \prod_{i=1}^M \\ &\quad \times \left(Q\left(\frac{\sqrt{\eta_i} + \mu_i}{\sigma_v}\right) + Q\left(\frac{\sqrt{\eta_i} - \mu_i}{\sigma_v}\right)\right). \end{aligned} \quad (14)$$

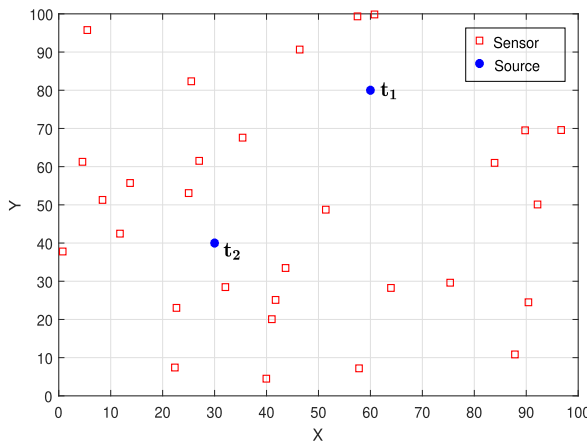


Fig. 2. Sample location of the sensors in the simulation. Two sources t_1 and t_2 are located at coordinates (60, 80) and (30, 40), respectively.

The values of η_i are determined using (13) based on the desired P_{fa_i} , given by $\eta_i = \sigma_v^2 [Q^{-1}((1/2)P_{\text{fa}_i})]^2$. This formula calculates η_i to control the false alarm probability at each recursion step.

V. SIMULATION RESULTS

We conducted a series of computer simulations to evaluate the performance of our proposed method. The simulations were conducted in a 100×100 m area. For each simulation run, we deployed a number of sensors (denoted by N) uniformly distributed across the field. All sensors were assumed to have $g_i = 1$. We set a fixed false alarm probability of 0.01 for all steps of the proposed method. Fig. 2 illustrates a sample scenario with $N = 30$ sensors.

The average Cramé(r)-Rao lower bound (rCRLB) is computed using (15), where $\mathbf{F}_{m,i}$ denotes the Fisher information matrix associated with the m th source in the i th simulation run

$$\text{CRLB} = \frac{1}{MN_t} \sum_{i=1}^{N_t} \sum_{m=1}^M \text{tr}(\mathbf{F}_{m,i}^{-1}). \quad (15)$$

Here, M denotes the total number of sources, and N_t signifies the overall number of Monte Carlo simulation runs. A detailed derivation of the CRLB can be found in [37]. In our simulations, we have compared the performance of the methods with the square root of the average CRLB, indicated by rCRLB. We also simulated the exhaustive search [36], the MR search method [36], and the EM algorithm [37] to compare their performance with our proposed algorithm. For the MR search method, we employed two-level grid resolutions of 4×4 m and 1×1 m. This implies that $[(100 \times 100)/(4 \times 4)]^M = 625^M$ and $[(4 \times 4)/(1 \times 1)]^M = 16^M$ grid points need to be searched in the two levels, respectively. Conversely, for the exhaustive search, the EM algorithm, and our proposed method, the grid size for the search is 1×1 . Consequently, for the exhaustive search, $[(100 \times 100)/(1 \times 1)]^M = 10^{4M}$ grid points are required to be searched. Given the high-computational complexity of the exhaustive search method, we constrained our analysis to scenarios with $M = 2$ and $M = 3$ sources. This limitation was imposed due to computational constraints beyond our capacity.

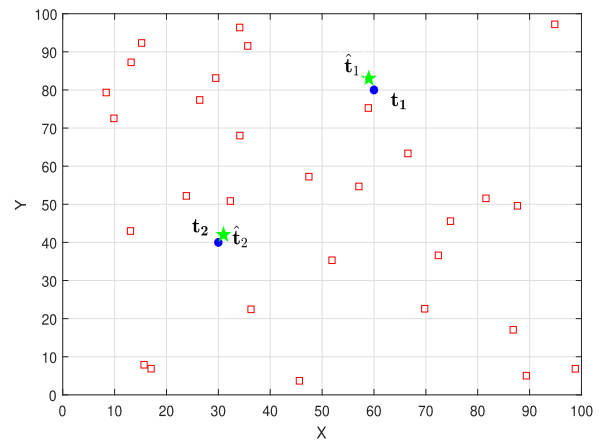


Fig. 3. Estimation of the source location using the proposed algorithm for $\sigma_v^2 = 1.5 \mu\text{W}$. Location of the sensors is marked by squares, and the estimated location of the sources is marked by stars.

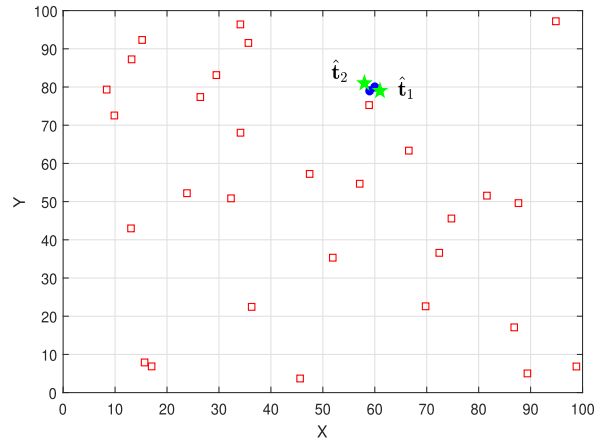


Fig. 4. Performance of the proposed method in a scenario where source #2 is close to source #1 for $\sigma_v^2 = 1.5 \mu\text{W}$. Location of the sensors is marked by squares, and the estimated location of the sources is marked by stars.

In Fig. 3, the positions of sources and sensors are depicted alongside a sample of estimated source numbers and their corresponding locations. In this particular scenario, two sources t_1 and t_2 are positioned at coordinates (60, 80) and (30, 40), respectively, with equal power levels $s_1 = s_2 = 1 \text{ mW}$, and a measurement noise variance of $\sigma_v^2 = 1.5$.

Fig. 4 illustrates a scenario where source t_2 is positioned at coordinates (59, 79), in close proximity to source t_1 . This simulation demonstrates the effectiveness of our proposed algorithm in accurately estimating the number and locations of even closely spaced sources.

We evaluated the performance of the mentioned location fixing methods using root-mean-square error (RMSE) as the metric. Fig. 5 shows the RMSE plotted against the noise variance σ_v^2 (in μW) for a fixed number of sensors ($N = 30$). Fig. 6 plots the RMSE against the number of sources (N) for a fixed noise variance ($\sigma_v^2 = 0.5$). In both simulations, we assumed two sources ($M = 2$) with equal power $s_1 = s_2 = 1 \text{ kW}$. Each data point in the figures represents the average result of 50 000 Monte Carlo simulation runs.

The performance of location methods is compared in Fig. 7 against the number of sources M . For this simulation, three

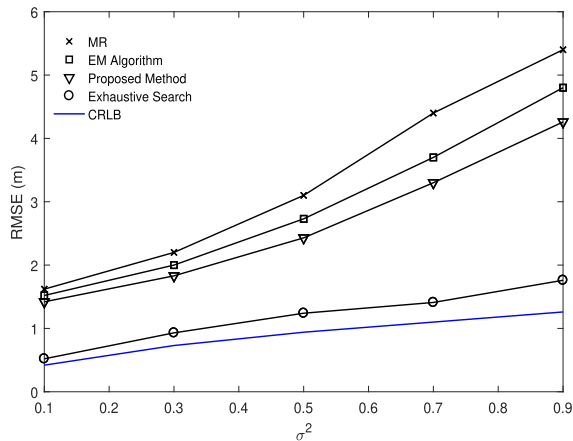


Fig. 5. Performance of the methods versus noise variance σ_v^2 (in μW) when $N = 30$ and $M = 2$. Each point of simulation is the average of 50k independent simulation runs.

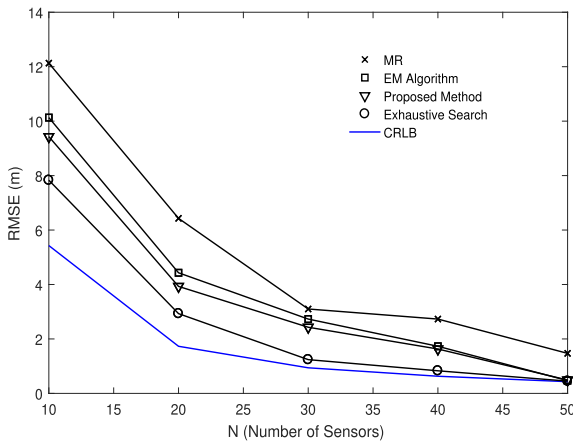


Fig. 6. Performance of the methods versus the number of sensors for $M = 2$ and $\sigma_v^2 = 0.5 \mu\text{W}$. Each point of simulation is the average of 50k independent simulation runs.

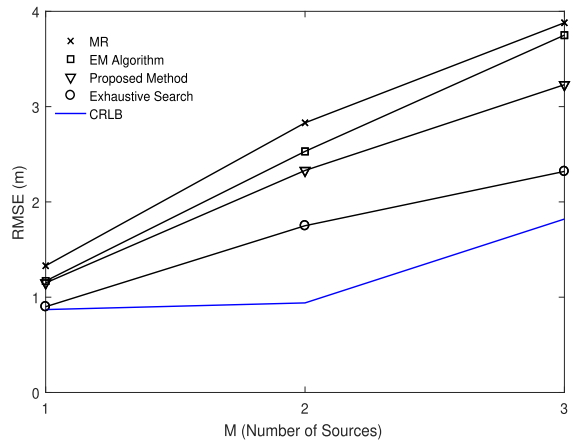


Fig. 7. Performance of the methods for $M = 1, 2$, and 3 sources with $N = 30$ and $\sigma_v^2 = 0.5 \mu\text{W}$. Each point of simulation is the average of 50k independent simulation runs.

sources t_1 , t_2 , and t_3 are positioned at $(10, 10)$, $(50, 50)$, and $(70, 70)$, with transmit powers $s_1 = s_2 = s_3 = 1 \text{ kW}$. We use $N = 30$ sensors, a noise variance of $\sigma_v^2 = 0.5$, and each data point represents the average of 50 000 Monte Carlo simulation runs. Notably, our proposed method consistently outperforms

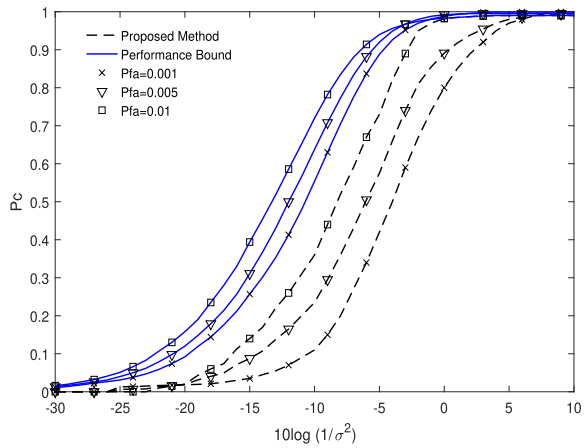


Fig. 8. Probability of correctly detecting the number of sources P_c versus $10\log(1/\sigma_v^2)$ for two sources.

TABLE II
COMPARISON OF COMPUTATIONAL COMPLEXITY AMONG METHODS

Method	Trials
Exhaustive search	$(100 \times 100)^M$
MR search ($4 \times 4, 1 \times 1$)	$(25 \times 25)^M + (4 \times 4)^M$
EM algorithm	$M (100 \times 100)$
Proposed algorithm	$M (100 \times 100)$

both the EM algorithm and the MR search method across all scenarios.

Fig. 8 illustrates the probability of correctly detecting the number of sources (P_c) using the proposed method. The x -axis represents the signal-to-noise ratio (SNR) in dB, plotted against $10\log(1/\sigma_v^2)$. This analysis considers three different false alarm probabilities: $P_{fa} = 0.001$, $P_{fa} = 0.005$, and $P_{fa} = 0.01$. The sources are positioned at coordinates $(60, 80)$ and $(30, 40)$, with transmit powers $s_1 = s_2 = 1 \text{ kW}$.

VI. COMPUTATIONAL COMPLEXITY COMPARISON

The proposed method, requiring no prior knowledge of the number of sources, significantly reduces computational complexity compared with both the exhaustive search and the MR search. **Table II** presents the number of iterations required for each algorithm.

VII. CONCLUSION

In this article, we presented a novel algorithm for estimating the number, locations, and transmit powers of wireless signal sources in a surveillance area based on RSS measurement. Our proposed method leverages sequential binary hypothesis testing, offering a computationally efficient solution without requiring prior knowledge of the number of sources. Through extensive simulations, we demonstrated the superior performance of our algorithm compared with the existing methods, such as the exhaustive search and the MR search, in terms of accuracy and computational complexity. One of the advantages of our proposed algorithm over the existing methods is that it does not need to have a foreknowledge about the number of sources.

Our results illustrate the robustness of the proposed algorithm in various scenarios, including cases with multiple sources and close proximity between them. In addition,

we conducted performance analysis to evaluate the algorithm's sensitivity to noise variance and false alarm probability, showcasing its reliability under different conditions.

Overall, our work contributes to the advancement of wireless signal processing techniques, particularly in scenarios where accurate source localization is crucial. Future research directions may include further optimization of the algorithm for real-time implementation and exploration of its applicability in diverse environments.

In conclusion, the proposed algorithm offers a promising solution for efficient and accurate estimation of wireless signal sources, paving the way for enhanced surveillance and monitoring capabilities in wireless communication systems.

APPENDIX A DERIVATION OF THE LIKELIHOOD RATIO

The SVD decomposition of \mathbf{D}_{m-1} with dimensions $N \times (m-1)$ is represented as (16), where $\mathbf{U}_2^T \mathbf{U}_2 = \mathbf{I}$ [48]

$$\mathbf{D}_{m-1} = [\mathbf{U}_1 \quad \mathbf{U}_2] \begin{bmatrix} \Sigma & \mathbf{0} \\ \mathbf{0} & \mathbf{0} \end{bmatrix} \begin{bmatrix} \mathbf{V}_1^T \\ \mathbf{V}_2^T \end{bmatrix}. \quad (16)$$

Here, \mathbf{U}_1 is an orthogonal matrix that its $(m-1)$ columns span the columns of \mathbf{D}_{m-1} , and \mathbf{U}_2 is a matrix with $(N-m+1)$ columns that lies in the null space of \mathbf{D}_{m-1}^T and is orthogonal to both \mathbf{U}_1 and \mathbf{D}_{m-1} . Therefore, we have $\mathbf{U}_2^T \mathbf{D}_{m-1} = \mathbf{0}$. Multiplying \mathbf{U}_2^T from the left to (4), we obtain

$$\begin{cases} H_{0,m} : \mathbf{p}_u = \mathbf{w}_u \\ H_{1,m} : \mathbf{p}_u = \mathbf{d}_m^u s_m + \mathbf{w}_u, \end{cases} \quad m = 1, 2, \dots, M \quad (17)$$

where $\mathbf{p}_u = \mathbf{U}_2^T \mathbf{p}$, $\mathbf{d}_m^u = \mathbf{U}_2^T \mathbf{d}_m$, and $\mathbf{w}_u = \mathbf{U}_2^T \mathbf{w}$.

Since $\mathbf{U}_2^T \mathbf{U}_2 = \mathbf{I}$, \mathbf{w}_u is a zero-mean Gaussian random vector with covariance matrix $\sigma_v^2 \mathbf{I}$.

To obtain the GLRT detector, the ML estimation of the unknown parameters must be calculated under hypotheses $H_{0,m}$ and $H_{1,m}$. From the above discussion, we have ($\Upsilon = 1/(2\pi\sigma_v^2)^{1/2})^{N-m+1}$)

$$f(\mathbf{p}_u; H_{0,m}) = \Upsilon e^{-\frac{1}{2\sigma_v^2} \|\mathbf{p}_u\|^2} \quad (18)$$

$$f(\mathbf{p}_u; H_{1,m}, s_m, x_m, y_m) = \Upsilon e^{-\frac{1}{2\sigma_v^2} \|\mathbf{p}_u - \mathbf{d}_m^u s_m\|^2}. \quad (19)$$

The ML estimation of the unknown parameters s_m and (x_m, y_m) under the assumption $H_{1,m}$ is as follows:

$$H_{1,m} : \begin{cases} \hat{s}_m = (\mathbf{d}_m^u)^\dagger \mathbf{p}_u = (\mathbf{d}_m^u)^T \mathbf{p}_u / \|\mathbf{d}_m^u\|^2 \\ (\hat{x}_m, \hat{y}_m) = \arg \max_{x_m, y_m} f(\mathbf{p}_u; H_{1,m}, \hat{s}_m, x_m, y_m). \end{cases} \quad (20)$$

By substituting (20) into (19), we obtain

$$f(\mathbf{p}_u; H_{1,m}, \hat{s}_m, x_m, y_m) = \Upsilon e^{-\frac{1}{2\sigma_v^2} \mathbf{p}_u^T (\mathbf{I} - \mathbf{d}_m^u (\mathbf{d}_m^u)^\dagger) \mathbf{p}_u}.$$

We also obtain

$$f(\mathbf{p}_u; H_{1,m}, \hat{s}_m, \hat{x}_m, \hat{y}_m) = \max_{x_m, y_m} \Upsilon e^{-\frac{1}{2\sigma_v^2} \mathbf{p}_u^T (\mathbf{I} - \mathbf{d}_m^u (\mathbf{d}_m^u)^\dagger) \mathbf{p}_u}.$$

The likelihood ratio $L_m(\mathbf{p})$ is calculated as follows:

$$L_m(\mathbf{p}) = \max_{x_m, y_m} \frac{f(\mathbf{p}_u; H_{1,m}, \hat{s}_m, \hat{x}_m, \hat{y}_m)}{f(\mathbf{p}_u; H_{0,m})}$$

$$\begin{aligned} &= \max_{x_m, y_m} \exp \left\{ \frac{1}{2\sigma_v^2} \left[\mathbf{p}_u^T \mathbf{d}_m^u (\mathbf{d}_m^u)^\dagger \mathbf{p}_u \right] \right\} \\ &= \max_{x_m, y_m} \frac{\|(\mathbf{d}_m^u)^T \mathbf{p}_u\|^2}{\|\mathbf{d}_m^u\|^2}. \end{aligned} \quad (21)$$

By substituting $\mathbf{p}_u = \mathbf{U}_2^T \mathbf{p}$ and $\mathbf{d}_m^u = \mathbf{U}_2^T \mathbf{d}_m$, we have

$$L_m(\mathbf{p}) = \max_{x_m, y_m} \frac{|\mathbf{d}_m^T \mathbf{U}_2 \mathbf{U}_2^T \mathbf{p}|^2}{\mathbf{d}_m^T \mathbf{U}_2 \mathbf{U}_2^T \mathbf{d}_m}. \quad (22)$$

Now, considering the relation $\mathbf{U}_2 \mathbf{U}_2^T = \mathbf{I} - \mathbf{D}_{m-1} \mathbf{D}_{m-1}^\dagger = \mathbf{D}_{m-1}^\perp$, we can express (22) as follows:

$$L_m(\mathbf{p}) = \max_{x_m, y_m} \left(\frac{|\mathbf{d}_m^T \mathbf{D}_{m-1}^\perp \mathbf{p}|^2}{\mathbf{d}_m^T \mathbf{D}_{m-1}^\perp \mathbf{d}_m} \right) \stackrel{H_{1,m}}{\gtrless} \eta_m. \quad (23)$$

Based on (20), the estimation of s_m is also calculated as follows:

$$\hat{s}_m = \frac{(\mathbf{d}_m^u)^T \mathbf{p}_u}{\|\mathbf{d}_m^u\|^2} = \frac{\mathbf{d}_m^T \mathbf{D}_{m-1}^\perp \mathbf{p}}{\mathbf{d}_m^T \mathbf{D}_{m-1}^\perp \mathbf{d}_m}. \quad (24)$$

In what follows, the clairvoyant detector [49] is also derived for (4). x_m , y_m , and s_m are assumed to be known in (19), and we have

$$\begin{aligned} f(\mathbf{p}_u; H_{0,m}) &= \Upsilon e^{-\frac{1}{2\sigma_v^2} \|\mathbf{p}_u\|^2} \\ f(\mathbf{p}_u; H_{1,m}) &= \Upsilon e^{-\frac{1}{2\sigma_v^2} \|\mathbf{p}_u - \mathbf{d}_m^u s_m\|^2}. \end{aligned} \quad (25)$$

Therefore, the likelihood ratio in this case is written as follows:

$$l_m(\mathbf{p}) = \frac{f(\mathbf{p}_u; H_{1,m})}{f(\mathbf{p}_u; H_{0,m})} = e^{-\frac{s_m^2 \|\mathbf{d}_m^u\|^2 - 2s_m \mathbf{p}_u^T \mathbf{d}_m^u}{2\sigma_v^2}} \stackrel{H_{1,m}}{\gtrless} \eta_m'' \quad (26)$$

where η_m'' is the threshold level adjusted for this step. $l_m(\mathbf{p})$ in (26) is equivalent as follows:

$$l_m(\mathbf{p}) = \exp \left\{ \frac{s_m}{\sigma_v^2} \mathbf{p}_u^T \mathbf{d}_m^u \right\} \stackrel{H_{1,m}}{\gtrless} \eta_m'. \quad (27)$$

Here, $\eta_m' = \eta_m'' e^{(s_m^2 \|\mathbf{d}_m^u\|^2)/(2\sigma_v^2)}$.

By taking logarithm of both sides of (27), we obtain

$$l_m(\mathbf{p}) = \mathbf{p}_u^T \mathbf{d}_m^u = \mathbf{d}_m^T \mathbf{D}_{m-1}^\perp \mathbf{p} \stackrel{H_{1,m}}{\gtrless} \eta_m \quad (28)$$

where $\eta_m = (\sigma_v^2 / s_m) \ln(\eta_m')$.

If s_m is assumed to be unknown and (x_m, y_m) is assumed to be known, the ML estimation of s_m from (24) is inserted into (27), and we will have

$$L_m(\mathbf{p}) = \left(\frac{|\mathbf{d}_m^T \mathbf{D}_{m-1}^\perp \mathbf{p}|^2}{\mathbf{d}_m^T \mathbf{D}_{m-1}^\perp \mathbf{d}_m} \right) \stackrel{H_{1,m}}{\gtrless} \eta_m. \quad (29)$$

Detector (29) is called a pseudo-clairvoyant detector, which is used to calculate an analytical performance bound for the probability of correctly detecting the number of sources.

APPENDIX B PROOF OF $L_i(\mathbf{p})$ AND $L_j(\mathbf{p})$ INDEPENDENCY

Theorem: For an N -dimensional complex vector \mathbf{z} with distribution $\mathcal{CN}(\mu, \mathbf{C})$ and for $N \times N$ dimensional Hermitian matrices \mathbf{B} and \mathbf{K} , if $\mathbf{BCK} = \mathbf{0}$, then the random variables $\mathbf{z}^H \mathbf{Bz}$ and $\mathbf{z}^H \mathbf{Kz}$ are independent [50]. \square

In our problem, $L_k(\mathbf{p})$ can be written in the quadratic form (30) in which $\varrho_k \stackrel{\text{def}}{=} (\mathbf{d}_k^T \mathbf{D}_{k-1}^\perp \mathbf{d}_k)^{-1}$ is independent of the observation vector $\mathbf{p} \sim \mathcal{N}(\mathbf{D}_M \mathbf{s}_M, \sigma_v^2 \mathbf{I})$

$$L_k(\mathbf{p}) = \varrho_k \mathbf{p}^T \mathbf{D}_{k-1}^\perp \mathbf{d}_k \mathbf{d}_k^T \mathbf{D}_{k-1}^\perp \mathbf{p}. \quad (30)$$

Now, for $\mathbf{B} = \mathbf{D}_{i-1}^\perp \mathbf{d}_i \mathbf{d}_i^T \mathbf{D}_{i-1}^\perp$ and $\mathbf{K} = \mathbf{D}_{j-1}^\perp \mathbf{d}_j \mathbf{d}_j^T \mathbf{D}_{j-1}^\perp$, with $\mathbf{C} = \sigma_v^2 \mathbf{I}$, $L_i(\mathbf{p})$ and $L_j(\mathbf{p})$ are independent for $i \neq j$ if $\mathbf{BK} = \mathbf{0}$.

This can be demonstrated using the properties $\mathbf{A}^\perp = \mathbf{I} - \mathbf{A}(\mathbf{A}^T \mathbf{A})^{-1} \mathbf{A}^T$, $\mathbf{D}_{j-1}^\perp \mathbf{D}_{j-1}^\perp = \mathbf{0}$, and $\mathbf{D}_{i-1}^\perp \mathbf{D}_{j-1}^\perp = \mathbf{0}$ (for $i < j$). Applying these, we derive

$$\mathbf{D}_{i-1}^\perp \mathbf{D}_{j-1}^\perp = \mathbf{D}_{j-1}^\perp, \quad \text{for } i < j. \quad (31)$$

Using (31) and the fact that $\mathbf{d}_i^T \mathbf{D}_{j-1}^\perp = \mathbf{0}$, we find

$$\mathbf{BK} = \mathbf{D}_{i-1}^\perp \mathbf{d}_i \mathbf{d}_i^T \mathbf{D}_{i-1}^\perp \mathbf{D}_{j-1}^\perp \mathbf{d}_j \mathbf{d}_j^T \mathbf{D}_{j-1}^\perp = \mathbf{0}.$$

APPENDIX C DISTRIBUTION FUNCTION OF $L_i(\mathbf{p})$

Since \mathbf{p} is a Gaussian random vector, then $\stackrel{\text{def}}{=} (\mathbf{d}_i^T \mathbf{D}_{i-1}^\perp \mathbf{p}) / ((\mathbf{d}_i^T \mathbf{D}_{i-1}^\perp \mathbf{d}_i)^{1/2})$ is Gaussian with distribution $\mathcal{N}(\mu_z, \sigma_z^2)$. Hence, $L_i(\mathbf{p}) = z_i^2$, and its distribution can be easily find to be (see [51, p. 132])

$$f_{L_i(\mathbf{p})}(x) = \frac{1}{\sqrt{8x\pi\sigma_z^2}} \left(e^{-\frac{(\sqrt{x}-\mu_z)^2}{2\sigma_z^2}} + e^{-\frac{(\sqrt{x}+\mu_z)^2}{2\sigma_z^2}} \right). \quad (32)$$

To calculate the mean and variance of z_i , let us rewrite \mathbf{p} for M sources as follows:

$$\mathbf{p} = \mathbf{D}_M \mathbf{s}_M + \mathbf{w}. \quad (33)$$

The mean and variance of z_i are calculated as follows:

$$\begin{aligned} E\{z_{M+1}\} &= \mathbf{d}_{M+1}^T \mathbf{D}_M^\perp E\{\mathbf{D}_M \mathbf{s}_M + \mathbf{w}\} / \sqrt{\mathbf{d}_{M+1}^T \mathbf{D}_M^\perp \mathbf{d}_{M+1}} \\ &= \frac{\mathbf{d}_{M+1}^T \mathbf{D}_M^\perp \mathbf{D}_M \mathbf{s}_M}{\sqrt{\mathbf{d}_{M+1}^T \mathbf{D}_M^\perp \mathbf{d}_{M+1}}} = 0 \end{aligned} \quad (34)$$

$$\begin{aligned} E\{z_i\} &= \mathbf{d}_i^T \mathbf{D}_{i-1}^\perp E\{\mathbf{D}_M \mathbf{s}_M + \mathbf{w}\} / \sqrt{\mathbf{d}_i^T \mathbf{D}_{i-1}^\perp \mathbf{d}_i}, \quad \text{for } i \leq M \\ &= \mathbf{d}_i^T \mathbf{D}_{i-1}^\perp \left(\sum_{k=1}^M s_k \mathbf{d}_k \right) / \sqrt{\mathbf{d}_i^T \mathbf{D}_{i-1}^\perp \mathbf{d}_i} \\ &= \mathbf{d}_i^T \mathbf{D}_{i-1}^\perp \left(\sum_{k=i}^M s_k \mathbf{d}_k \right) / \sqrt{\mathbf{d}_i^T \mathbf{D}_{i-1}^\perp \mathbf{d}_i} \\ &= \sum_{k=i}^M s_k \mathbf{d}_k^T \mathbf{D}_{i-1}^\perp \mathbf{d}_k / \sqrt{\mathbf{d}_i^T \mathbf{D}_{i-1}^\perp \mathbf{d}_i} \end{aligned} \quad (35)$$

$$\begin{aligned} \sigma_v^2 \{z_i\} &= E \left\{ \frac{\mathbf{d}_i^T \mathbf{D}_{i-1}^\perp \mathbf{w} \mathbf{w}^T \mathbf{D}_{i-1}^\perp \mathbf{d}_i}{\mathbf{d}_i^T \mathbf{D}_{i-1}^\perp \mathbf{d}_i} \right\} \\ &= \frac{\mathbf{d}_i^T \mathbf{D}_{i-1}^\perp E\{\mathbf{w} \mathbf{w}^T\} \mathbf{D}_{i-1}^\perp \mathbf{d}_i}{\mathbf{d}_i^T \mathbf{D}_{i-1}^\perp \mathbf{d}_i} = \sigma_v^2. \end{aligned} \quad (36)$$

In which, \mathbf{D}_{i-1}^\perp is idempotent, and \mathbf{w} is $\mathcal{N}(\mathbf{0}, \sigma_v^2 \mathbf{I})$. Hence, the followings can be expressed:

$$z_i \sim \mathcal{N}(0, \sigma_v^2), \quad \text{for } i = M + 1 \quad (37)$$

$$z_i \sim \mathcal{N} \left(\frac{\sum_{k=i}^M s_k \mathbf{d}_k^T \mathbf{D}_{i-1}^\perp \mathbf{d}_k}{\sqrt{\mathbf{d}_i^T \mathbf{D}_{i-1}^\perp \mathbf{d}_i}}, \sigma_v^2 \right), \quad \text{for } i \leq M. \quad (38)$$

ACKNOWLEDGMENT

The authors would like to thank the Associate Editor and the referees for their valuable time, insightful comments, and constructive suggestions, which have significantly contributed to the improvement of this article.

REFERENCES

- [1] H. Wymeersch, J. Lien, and M. Z. Win, "Cooperative localization in wireless networks," *Proc. IEEE*, vol. 97, no. 2, pp. 427–450, Feb. 2009.
- [2] Z. Dai, G. Wang, and H. Chen, "Sensor selection for TDOA-based source localization using angle and range information," *IEEE Trans. Aerosp. Electron. Syst.*, vol. 57, no. 4, pp. 2597–2604, Aug. 2021.
- [3] E. Xu, Z. Ding, and S. Dasgupta, "Source localization in wireless sensor networks from signal time-of-arrival measurements," *IEEE Trans. Signal Process.*, vol. 59, no. 6, pp. 2887–2897, Jun. 2011.
- [4] J. A. D. Peral-Rosado, R. Raulefs, J. A. López-Salcedo, and G. Seco-Granados, "Survey of cellular mobile radio localization methods: From 1G to 5G," *IEEE Commun. Surveys Tuts.*, vol. 20, no. 2, pp. 1124–1148, 2nd Quart., 2017.
- [5] X. Su, I. Ullah, X. Liu, and D. Choi, "A review of underwater localization techniques, algorithms, and challenges," *J. Sensors*, vol. 2020, pp. 1–24, Jan. 2020.
- [6] H. Godrich, A. M. Haimovich, and R. S. Blum, "Target localization accuracy gain in MIMO radar-based systems," *IEEE Trans. Inf. Theory*, vol. 56, no. 6, pp. 2783–2803, Jun. 2010.
- [7] L. Yan, L. Pallotta, G. Giunta, and D. Orlando, "Robust target localization for multistatic passive radar networks," *IEEE Sensors Lett.*, vol. 7, no. 7, pp. 1–4, Jul. 2023.
- [8] M. Sedighizad, B. Seyfe, and S. Valaei, "A correntropy based algorithm for robust localization in wireless networks," in *Proc. IEEE Int. Conf. Acoust., Speech Signal Process. (ICASSP)*, Jun. 2021, pp. 4660–4664.
- [9] F. Keyrouz, "Advanced binaural sound localization in 3-D for humanoid robots," *IEEE Trans. Instrum. Meas.*, vol. 63, no. 9, pp. 2098–2107, Sep. 2014.
- [10] I. Guvenc and C.-C. Chong, "A survey on TOA based wireless localization and NLOS mitigation techniques," *IEEE Commun. Surveys Tuts.*, vol. 11, no. 3, pp. 107–124, 3rd Quart., 2009.
- [11] W. Wang, G. Wang, J. Zhang, and Y. Li, "Robust weighted least squares method for TOA-based localization under mixed LOS/NLOS conditions," *IEEE Commun. Lett.*, vol. 21, no. 10, pp. 2226–2229, Oct. 2017.
- [12] B. Huang, L. Xie, and Z. Yang, "TDOA-based source localization with distance-dependent noises," *IEEE Trans. Wireless Commun.*, vol. 14, no. 1, pp. 468–480, Jan. 2015.
- [13] K. C. Ho, "Bias reduction for an explicit solution of source localization using TDOA," *IEEE Trans. Signal Process.*, vol. 60, no. 5, pp. 2101–2114, May 2012.
- [14] A. Amar and A. J. Weiss, "Localization of narrowband radio emitters based on Doppler frequency shifts," *IEEE Trans. Signal Process.*, vol. 56, no. 11, pp. 5500–5508, Nov. 2008.
- [15] H.-J. Shao, X.-P. Zhang, and Z. Wang, "Efficient closed-form algorithms for AOA based self-localization of sensor nodes using auxiliary variables," *IEEE Trans. Signal Process.*, vol. 62, no. 10, pp. 2580–2594, May 2014.
- [16] Y. Sun, K. C. Ho, and Q. Wan, "Eigenspace solution for AOA localization in modified polar representation," *IEEE Trans. Signal Process.*, vol. 68, pp. 2256–2271, 2020.
- [17] M. Biguesh and S. Gazor, "On proper antenna pattern for a simple source detection and localization system," *IEEE Trans. Antennas Propag.*, vol. 57, no. 4, pp. 1073–1080, Apr. 2009.
- [18] F. Pang, K. Dogancay, H. Wang, and X. Shen, "Bias compensation method for 3-D AOA-TMA with uncertainty in sensor positions," *IEEE Sensors J.*, vol. 24, no. 9, pp. 14482–14492, May 2024.

- [19] J. Yin, Q. Wan, S. Yang, and K. C. Ho, "A simple and accurate TDOA-AOA localization method using two stations," *IEEE Signal Process. Lett.*, vol. 23, no. 1, pp. 144–148, Jan. 2016.
- [20] X. Li, "RSS-based location estimation with unknown pathloss model," *IEEE Trans. Wireless Commun.*, vol. 5, no. 12, pp. 3626–3633, Dec. 2006.
- [21] Q. Wang, Z. Duan, and X. R. Li, "Three-dimensional location estimation using biased RSS measurements," *IEEE Trans. Aerosp. Electron. Syst.*, vol. 56, no. 6, pp. 4673–4688, Dec. 2020.
- [22] L. A. Caceres Najarro, I. Song, and K. Kim, "Differential evolution with opposition and redirection for source localization using RSS measurements in wireless sensor networks," *IEEE Trans. Autom. Sci. Eng.*, vol. 17, no. 4, pp. 1736–1747, Oct. 2020.
- [23] M. Zhou, Y. Li, M. J. Tahir, X. Geng, Y. Wang, and W. He, "Integrated statistical test of signal distributions and access point contributions for Wi-Fi indoor localization," *IEEE Trans. Veh. Technol.*, vol. 70, no. 5, pp. 5057–5070, May 2021.
- [24] H. Katabalian, M. Biguesh, and A. Sheikhi, "A closed-form solution for localization based on RSS," *IEEE Trans. Aerosp. Electron. Syst.*, vol. 56, no. 2, pp. 912–923, Apr. 2020.
- [25] A. Heydari, M. Aghabozorgi, and M. Biguesh, "Optimal sensor placement for source localization based on RSSD," *Wireless Netw.*, vol. 26, no. 7, pp. 5151–5162, Oct. 2020.
- [26] S. Xu, "Optimal sensor placement for target localization using hybrid RSS, AOA and TOA measurements," *IEEE Commun. Lett.*, vol. 24, no. 9, pp. 1966–1970, Sep. 2020.
- [27] K. C. Ho and W. Xu, "An accurate algebraic solution for moving source location using TDOA and FDOA measurements," *IEEE Trans. Signal Process.*, vol. 52, no. 9, pp. 2453–2463, Sep. 2004.
- [28] J. Li, K. Dogancay, and H. Hmam, "Closed-form pseudolinear estimators for DRSS-AOA localization," *Sensors*, vol. 21, no. 21, p. 7159, Oct. 2021.
- [29] A. Coluccia and F. Ricciato, "On ML estimation for automatic RSS-based indoor localization," in *Proc. IEEE 5th Int. Symp. Wireless Pervasive Comput.*, May 2010, pp. 495–502.
- [30] R. W. Ouyang, A. K.-S. Wong, and C.-T. Lea, "Received signal strength-based wireless localization via semidefinite programming: Non-cooperative and cooperative schemes," *IEEE Trans. Veh. Technol.*, vol. 59, no. 3, pp. 1307–1318, Mar. 2010.
- [31] S. Tomic, M. Beko, and R. Dinis, "RSS-based localization in wireless sensor networks using convex relaxation: Noncooperative and cooperative schemes," *IEEE Trans. Veh. Technol.*, vol. 64, no. 5, pp. 2037–2050, May 2015.
- [32] H. C. So and L. Lin, "Linear least squares approach for accurate received signal strength based source localization," *IEEE Trans. Signal Process.*, vol. 59, no. 8, pp. 4035–4040, Aug. 2011.
- [33] J. H. Lee and R. M. Buehrer, "Location estimation using differential RSS with spatially correlated shadowing," in *Proc. GLOBECOM IEEE Global Telecommun. Conf.*, Nov. 2009, pp. 1–6.
- [34] B.-C. Liu and K.-H. Lin, "SSSD-based mobile positioning: On the accuracy improvement issues in distance and location estimations," *IEEE Trans. Veh. Technol.*, vol. 58, no. 3, pp. 1245–1254, Mar. 2009.
- [35] S. D. Chitte and S. Dasgupta, "Distance estimation from received signal strength under log-normal shadowing: Bias and variance," in *Proc. 9th Int. Conf. Signal Process.*, vol. 55, Oct. 2008, pp. 256–259.
- [36] X. Sheng and Y.-H. Hu, "Maximum likelihood multiple-source localization using acoustic energy measurements with wireless sensor networks," *IEEE Trans. Signal Process.*, vol. 53, no. 1, pp. 44–53, Jan. 2005.
- [37] W. Meng, W. Xiao, and L. Xie, "An efficient EM algorithm for energy-based multisource localization in wireless sensor networks," *IEEE Trans. Instrum. Meas.*, vol. 60, no. 3, pp. 1017–1027, Mar. 2011.
- [38] M. Wax and I. Ziskind, "Detection of the number of coherent signals by the MDL principle," *IEEE Trans. Acoust., Speech, Signal Process.*, vol. 37, no. 8, pp. 1190–1196, Aug. 1989.
- [39] M. Wax and A. Adler, "Detection of the number of signals by signal subspace matching," *IEEE Trans. Signal Process.*, vol. 69, pp. 973–985, 2021.
- [40] M. Wax and T. Kailath, "Detection of signals by information theoretic criteria," *IEEE Trans. Acoust., Speech, Signal Process.*, vol. ASSP-33, no. 2, pp. 387–392, Apr. 1985.
- [41] J. Högbom, "Aperture synthesis with a non-regular distribution of interferometer baselines," *Astron. Astrophys.*, vol. 15, p. 417, Jun. 1974.
- [42] T. T. Cao and L. Rosenberg, "An improved clean algorithm for ISAR," in *Proc. IEEE Radar Conf. (RadarConf)*, Mar. 2022, pp. 1–6.
- [43] A. Goldsmith, *Wireless Communications*. Cambridge, U.K.: Cambridge Univ. Press, 2005.
- [44] S. Uluskan, "Maximum correlation coefficient estimation (MCORE): A new estimation philosophy for RSS based target localization," *Signal Process.*, vol. 178, Jan. 2021, Art. no. 107814.
- [45] L. L. Scharf and B. Friedlander, "Matched subspace detectors," *IEEE Trans. Signal Process.*, vol. 42, no. 8, pp. 2146–2157, Aug. 1994.
- [46] F. Izedi, M. Karimi, and M. Derakhtian, "Joint DOA estimation and source number detection for arrays with arbitrary geometry," *Signal Process.*, vol. 140, pp. 149–160, Nov. 2017.
- [47] J. Zhu, H. Zhang, N. Zhang, J. Fang, and F. Qu, "Line spectrum estimation and detection with few-bit ADCs: Theoretical analysis and generalized NOMP algorithm," 2023, *arXiv:2307.00491*.
- [48] C. D. Meyer, *Matrix Analysis and Applied Linear Algebra*, vol. 71. Philadelphia, PA, USA: SIAM, 2000.
- [49] S. M. Kay, *Fundamentals of Statistical Signal Processing: Detection Theory*. Upper Saddle River, NJ, USA: Prentice-Hall, 1998.
- [50] G. R. C. Alvin and S. Bruce, *Linear Models in Statistics*. Hoboken, NJ, USA: Wiley, 2008, ch. 4.
- [51] A. Papoulis and S. U. Pillai, *Probability, Random Variables, and Stochastic Processes*. New York, NY, USA: McGraw-Hill, 2002.



Hamid Katabalian was born in Hamedan, Iran. He received the B.Sc. (Hons.) degree in electrical engineering from Zanjan University, Zanjan, Iran, in 2012, and the M.Sc. and Ph.D. (Hons.) degrees in communication systems from Shiraz University, Shiraz, Iran, in 2014 and 2022, respectively.

His main research interests include statistical signal processing, detection theory, source localization, and array signal processing.



Mehrzad Biguesh (Bighesh) is a Professor with the Department of Communications and Electronics, Shiraz University, Shiraz, Iran. From 2002 to 2004, he was a Postdoctoral Fellow and a Senior Researcher at the University of Duisburg-Essen, Essen, Germany. From 2004 to 2011, he served as a Visiting Professor at Queen's University, Kingston, ON, Canada, and the University of Toronto, Toronto, ON, Canada, on several occasions. He has substantial industrial experience, contributing to projects at Esprooz Special Processing Company, Shiraz, and other organizations. His research interests include signal processing, wireless communications, array signal processing, channel estimation, localization in wireless systems, and sensor arrays.



Abbass Sheikhi was born in Shiraz, Iran, in 1971. He received the B.Sc. degree in electronics engineering from Shiraz University, Shiraz, in 1993, and the M.Sc. (Hons.) degree in biomedical engineering and the Ph.D. (Hons.) degree in communications engineering from Sharif University of Technology, Tehran, Iran, in 1995 and 1999, respectively.

Since 1999, he has been with the Department of Electrical and Electronics Engineering, Shiraz University, where he currently a Professor. His current research interests include detection, estimation, and radar signal and data processing.